Plasmon polaritons in photonic superlattices containing a left-handed material

E. Reyes-Gómez[1], A. Bruno-Alfonso[2], S. B. Cavalcanti[3,4], C. A. A. de Carvalho[4,5], and L. E. Oliveira[4,6]
[1] *Instituto de Física, Universidad de Antioquia, AA 1226, Medellín, Colombia*
[2] *Faculdade de Ciências, UNESP - Universidade Estadual Paulista, 17033-360, Bauru-SP, Brazil*
[3] *Instituto de Física, UFAL, Cidade Universitária, 57072-970, Maceió-AL, Brazil*
[4] *Inmetro, Campus de Xerém, Duque de Caxias-RJ, 25250-020, Brazil*
[5] *Instituto de Física, UFRJ, Rio de Janeiro-RJ, 21945-972, Brazil*
[6] *Instituto de Física, UNICAMP, CP 6165, Campinas-SP, 13083-970, Brazil*
(Dated: July 9, 2009)

We analyze one-dimensional photonic superlattices which alternate layers of air and a left-handed material. We assume Drude-type dispersive responses for the dielectric permittivity and magnetic permeability of the left-handed material. Maxwell's equations and the transfer-matrix technique are used to derive the dispersion relation for the propagation of obliquely incident optical fields. The photonic dispersion indicates that the growth-direction component of the electric (or magnetic) field leads to the propagation of electric (or magnetic) plasmon polaritons, for either TE or TM configurations. Furthermore, we show that if the plasma frequency is chosen within the photonic $\langle n(\omega)\rangle = 0$ zeroth-order bandgap, the coupling of light with plasmons weakens considerably. As light propagation is forbidden in that particular frequency region, the plasmon-polariton mode reduces to a pure plasmon mode.

Keywords: photonics, superlattices, plasmon polaritons

PACS numbers: PACS: 41.20.Jb, 42.70.Gi, 42.70.Qs, and 78.20.Bh

Over the years, artificial complex materials have been increasingly used to shape and manipulate light[1,2,3,4,5]. The microstructuring of high quality optical materials yields remarkable flexibility in the fabrication of nanostructures, and allows for the tailoring of electromagnetic dispersions and mode structures to suit almost any need. Metamaterials[6,7,8,9,10,11,12,13], also known as left-handed materials (LHMs), are a remarkable example of such nanostructuring. Light propagation through metamaterials is characterized by a phase velocity opposite to the Poyinting vector, which corresponds to negative dispersive electric and magnetic responses.

The advent of metamaterials has opened a new era for optical devices, and has also given considerable thrust to the recent area of plasmonics, the study of plasmon polaritons. In metal-dielectric interfaces, for example, surface-plasmon polaritons are coupled modes that result from resonant interactions between electromagnetic waves and mobile electrons at the surface of a metal or semiconductor. Such resonant surface-plasmon polaritons may have much shorter wavelengths than that of the radiation, which enables them to propagate along nanoscale systems[1,2,3,4], opening up a wide range of possibilities for the construction of new optical devices. It is well known, for example, that one of the most important features of surface-plasmon polaritons is to confine light to very small dimensions, yielding the merging of photonics and electronics at the nanoscale. Furthermore, considering the dispersive character of the LHM's, together with the enhanced optical magnetism exhibited by them, one might conjecture the existence of remarkable new phenomena such as the excitation of plasmon polaritons of a magnetic nature, that is, magnetic density waves resulting from resonant interactions between the optical field and current densities at the metamaterial. Ultimately, those developments could lead to increases in the resolution of microscopes, in the efficiency of LEDs, and in the sensitivity of chemical and biological devices[5,6,7,8].

One-dimensional (1D) superlattices which alternate layers of positive and negative materials have already exhibited many interesting properties[14,15,16,17,18,19,20,21,22,23] that are absent in superlattices composed solely of positive materials. In particular, the existence of a non-Bragg photonic bandgap, also known as a zeroth order gap, has been suggested[12], detected[13,14], and characterized[15,16]. In order to investigate the possibility of excitation of electric/magnetic plasmon polaritons, in the present work we study the oblique incidence of light on a model 1D superlattice composed of layers A of air, and layers B of a doubly negative material. Layers A (width a) and B (width b) are distributed periodically so that $d = a + b$ is the period of the superlattice nanostructure (cf. Fig. 1).

In the B layers, the electric and magnetic responses are dispersive and may assume negative values. If one neglects losses, they may be described by[9,10,11,12,13]

$$\varepsilon_B(\omega) = \varepsilon_0 - \frac{\omega_e^2}{\omega^2} \;\; ; \;\; \mu_B(\omega) = \mu_0 - \frac{\omega_m^2}{\omega^2}\,, \qquad (1)$$

where $\varepsilon_B(\omega)$ and $\mu_B(\omega)$ are the dielectric permittivity and magnetic permeability in slab B, respectively, one may choose[10,11] $\varepsilon_0 = 1.21$ and $\mu_0 = 1.0$, and the electric/magnetic plasmon modes are at $\nu = \nu_e = \frac{\omega_e}{2\pi\sqrt{\epsilon_0}}$ and $\nu = \nu_m = \frac{\omega_m}{2\pi\sqrt{\mu_0}}$, which correspond to the solutions of $\epsilon_B(\omega) = 0$ and $\mu_B(\omega) = 0$, respectively.

We note that dispersions such as those in (1) hold in periodically LC loaded transmission lines[10]. These

negative-index systems were shown to exhibit good microwave properties, with low loss and broad bandwidth[11].

We shall be interested in studying the properties of both the transverse-electric (TE: electric field parallel to the interface plane, see Fig. 1) and transverse-magnetic (TM: magnetic field parallel to the interface) polarizations of a monochromatic electromagnetic field of frequency ω propagating through a 1D periodic system.

In the case of a TE field, one may choose

$$\mathbf{E}(\mathbf{r},t) = E(z)\exp\left[i\left(qx-\omega t\right)\right]\mathbf{e}_y\,, \qquad (2)$$

whereas, in the case of TM polarization, the magnetic field may be considered as

$$\mathbf{H}(\mathbf{r},t) = H(z)\exp\left[i\left(qx-\omega t\right)\right]\mathbf{e}_y, \qquad (3)$$

where we have assumed that the superlattice was grown along the z axis, q is the wavevector component along the x direction, and $\mathbf{e}_y$ is the cartesian unitary vector along the y direction.

Maxwell's equations lead to the following differential equations for the electric and magnetic amplitudes

$$\frac{d}{dz}\left[\frac{1}{\mu(z)}\frac{d}{dz}E(z)\right] = -\epsilon(z)\left[\left(\frac{\omega}{c}\right)^2 - \frac{q^2}{n^2(z)}\right]E(z), \quad (4)$$

and

$$\frac{d}{dz}\left[\frac{1}{\epsilon(z)}\frac{d}{dz}H(z)\right] = -\mu(z)\left[\left(\frac{\omega}{c}\right)^2 - \frac{q^2}{n^2(z)}\right]H(z), \quad (5)$$

where $n(z) = \sqrt{\epsilon(z)}\sqrt{\mu(z)}$ is the z-position dependent refraction index.

In the sequel, n_A and n_B are the refraction indices, while μ_A and μ_B are the magnetic permeabilities in layers A and B, respectively. Note that, because of (1), the n_B refraction index in layer B is a function of the frequency, and may be a real positive, real negative or a pure imaginary number. Also, note that q, the incident wavevector component along the x direction, may be obtained as a function of the angle of incidence $\theta \equiv \theta_A$ by $q = \frac{\omega}{c}n_A\sin\theta$.

Equations (4) and (5) may be solved by means of the transfer-matrix technique (see, for example, the work by Cavalcanti *et al*[16] and references therein). For n_B a real number, and $n_B^2 - n_A^2\sin^2\theta \geq 0$, the procedure yields the TE polarization dispersion relation from the solution of the transcendental equation

$$\begin{aligned}\cos(kd) &= \cos(Q_A a)\cos(Q_B b) \\ &\quad -\frac{1}{2}\left(\frac{F_A}{F_B}+\frac{F_B}{F_A}\right)\sin(Q_A a)\sin(Q_B b). \quad (6)\end{aligned}$$

In the formula, k is the Bloch wavevector along the z direction which is the axis of the photonic crystal; fields in consecutive unit cells are related by the Bloch condition, i.e., by the phase factor $e^{\,i\,k\,d}$. Q_A and Q_B are defined as

$$Q_A = \frac{\omega}{c}n_A|\cos\theta| = \frac{\omega}{c}n_A|\cos\theta_A|, \qquad (7)$$

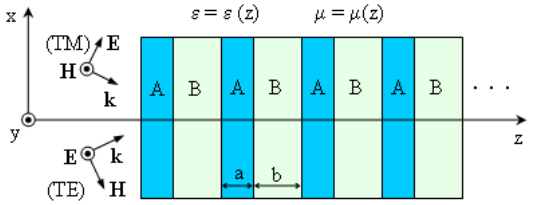

FIG. 1: (Color online) Pictorial view of the 1D multilayer photonic superlattice with layers A and B in periodic arrangement, and the electric and magnetic fields for the TE-like and TM-like electromagnetic waves schematically shown. Note that, for normal incidence, the two polarizations are equivalent.

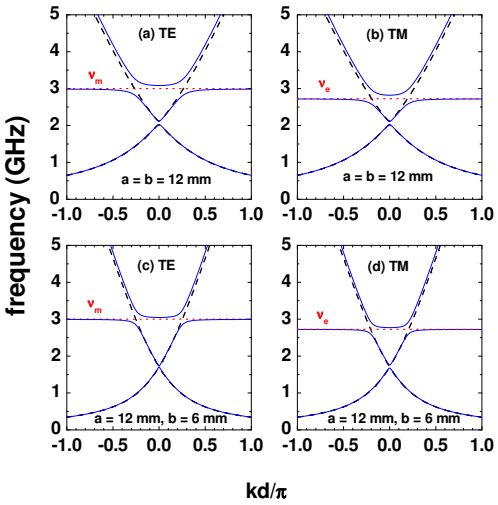

FIG. 2: (Color online) TE and TM dispersion relations $\nu = \nu(k)$ in photonic periodic superlattices ($\nu = \frac{\omega}{2\pi}$). Calculations were performed for air as slab A ($\epsilon_A = 1$, $\mu_A = 1$), $a = b = 12$ mm (also for $a = 12$ mm and $b = 6$ mm), and $\omega_e/2\pi = \omega_m/2\pi = 3$ GHz for the Drude model [cf. Eq. (1)] in slab B. Dotted lines indicate the pure electric/magnetic plasmon modes at $\nu = \nu_e = \frac{\omega_e}{2\pi\sqrt{\epsilon_0}}$ and $\nu = \nu_m = \frac{\omega_m}{2\pi\sqrt{\mu_0}}$. Solid and dashed lines correspond to $\theta = \pi/12$ and $\theta = 0$ incidence angles, respectively.

and

$$Q_B = \frac{\omega}{c}\sqrt{n_B^2 - n_A^2\sin^2\theta} = \frac{\omega}{c}|n_B||\cos\theta_B|, \qquad (8)$$

where, $F_A = (Q_A/\mu_A)$, $F_B = (Q_B/\mu_B)$ and, in the last equality, we have made use of Snell's law $n_A\sin\theta = n_B\sin\theta_B$.

For n_B a real number, and $n_B^2 - n_A^2\sin^2\theta < 0$, the procedure yields the TE polarization dispersion relation from the solution of the transcendental equation

$$\begin{aligned}\cos(kd) &= \cos(Q_A a)\cosh(Q_B b) \\ &\quad -\frac{1}{2}\left(\frac{F_A}{F_B}-\frac{F_B}{F_A}\right)\sin(Q_A a)\sinh(Q_B b). \quad (9)\end{aligned}$$

where Q_A is still given by (7), but

$$Q_B = \frac{\omega}{c}\sqrt{n_A^2\sin^2\theta - n_B^2}. \qquad (10)$$

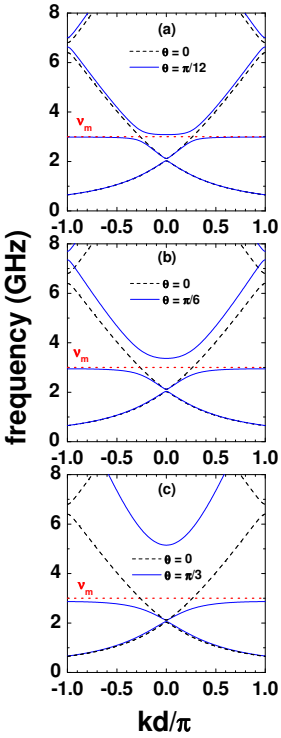

FIG. 3: (Color online) TE dispersion relations $\nu = \nu(k)$ in photonic periodic superlattices ($\nu = \frac{\omega}{2\pi}$) as functions of various incidence angles. Calculations were performed using the same parameters as in Fig. 2. Dotted lines indicate the pure magnetic plasmon modes at $\nu = \nu_m = \frac{\omega_m}{2\pi\sqrt{\mu_0}}$, dashed lines correspond to $\theta = 0$, and solid lines correspond to (a) $\theta = \pi/12$, (b) $\theta = \pi/6$ and (c) $\theta = \pi/3$ incidence angles, respectively.

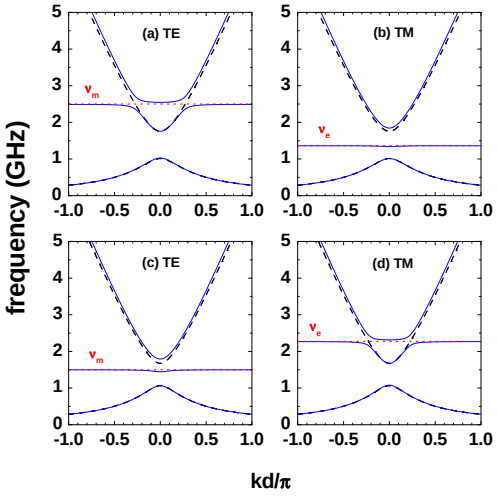

FIG. 4: (Color online) TE and TM dispersions in a photonic periodic superlattice with $a = b = 12$ mm. Numerical calculations were carried out for air as slab A ($\epsilon_A = 1$ and $\mu_A = 1$). For slab B, ϵ_B and μ_B were chosen by taking plasma frequencies in the Drude model as $\omega_e/2\pi = 1.5$ GHz and $\omega_m/2\pi = 2.5$ GHz, respectively, in (a) and (b), whereas in (c) and (d) we have taken $\omega_e/2\pi = 2.5$ GHz and $\omega_m/2\pi = 1.5$ GHz. Note that, in panel (b), the electric plasmon frequency $\nu_e = \frac{\omega_e}{2\pi\sqrt{\epsilon_0}}$ is in the $\langle n(\omega)\rangle = 0$ zeroth-order bandgap region, leading to a basically flat $\theta = \pi/12$ plasmon-polariton band with a frequency essentially equal to ν_e for the TM dispersion. A similar situation is observed for the TE dispersion in (c), as $\nu_m = \frac{\omega_m}{2\pi\sqrt{\mu_0}}$ falls in the zeroth-order gap region. Solid and dashed lines correspond to $\theta = \pi/12$ and $\theta = 0$ incidence angles, respectively.

Moreover, if $n_B^2 < 0$, (9) is still valid, with Q_A still given by (7), but

$$Q_B = \frac{\omega}{c}\sqrt{n_{BI}^2 - n_A^2 \sin^2\theta}, \qquad (11)$$

where n_{BI} is the imaginary part of n_B.

For the TM polarization, the transcendental equations (6) and (9), as well as the definitions of Q_A and Q_B for the different cases are also valid, provided one replaces μ_A by ϵ_A and μ_B by ϵ_B, where ϵ_A and ϵ_B are the dielectric permissivities in layers A and B, respectively.

Figure 2 shows the calculated dispersions ($\nu = \frac{\omega}{2\pi}$) in the cases of TE [Figs. 2(a) and 2(c)] and TM [Figs. 2(b) and 2(d)] polarizations, for different layer widths. Note that ν_e and ν_m fall outside the $\langle n(\omega)\rangle = 0$ zeroth order bandgap. For $\theta = 0$ (dashed curves), the second photonic band, just above the $\langle n(\omega)\rangle = 0$ zeroth order gap, is a pure photonic mode and, for $\theta = \pi/12$, there is a coupling between the radiation field and a plasmon mode which leads to a pair of plasmon-polariton modes. In other words, while for normal incidence the band just above the zeroth order gap is a pure photonic mode, for oblique incidence ($\theta \neq 0$) the *electromagnetic field + plasmon* interaction leads to a pair of coupled modes. We emphasize that, for $\theta = 0$, the electric- and magnetic-field components along the z growth direction are null and there is no longitudinal wave propagation. On the other hand, for $\theta \neq 0$, in the case of the TM (TE) configuration, the electric (magnetic) field has a component on the z direction, which results in the excitation of longitudinal electric (magnetic) waves. For $\theta = \pi/12$, Figure 2 illustrates that the pair of plasmon-polariton bands are asymptotic to the $\nu = \nu_e$ and $\nu = \nu_m$ pure electric/magnetic plasmon values. It is clear from Fig. 2 (a), for example, that at small values of k, the lowest $\theta = \pi/12$ plasmon-polariton mode behaves like an electromagnetic photonic wave. As k increases, the dispersion bends over and reaches the limiting value of the pure magnetic plasmon. On the other hand, the second $\theta = \pi/12$ plasmon-polariton branch behaves like a magnetic plasmon wave, at small k, and like an electromagnetic photonic mode as k increases. The same comments are valid for the other panels in Fig. 2 [of course, in the cases of Figs. 2(b) and 2(d), the electric plasmon mode is the one involved]. By comparing the results for normal and oblique incidence, it is clear that, for $\theta \neq 0$, resonant plasmon-polariton waves are excited by the coupling of the electric (or magnetic) plasmon modes with the incident eletromagnetic field. One may infer that

the plasmon-polariton waves are excited by the magnetic field, in the TE case, or driven by the electric field, in the TM case. This is consistent with the fact that those longitudinal waves, in the TE case, are asymptotic to the ν_m pure magnetic plasmon frequency whereas, in the TM case, the plasmon-polariton bands are asymptotic to the ν_e pure electric plasmon mode.

The calculated dispersions, for TE modes, as a function of the incidence angles are displayed in Fig. 3. We notice that the essential features persist irrespective of the incidence angle, although the Bragg gaps widens considerably for higher incidence angles. Also, Fig. 4 clearly indicates that, by choosing the resonant plasmon frequency within the $\langle n(\omega)\rangle = 0$ zeroth order bandgap, the coupling of light to plasmon modes, for $\theta \neq 0$, essentially disappears leading to a basically pure (electric or magnetic) plasmon mode. This is a consequence of the fact that the energy of the incident electromagnetic wave lies in a forbidden energy gap region and, therefore, the coupling of the incident light with plasmons is expected to be quite weak.

Summing up, we have studied light propagation through a 1D superlattice composed of alternate layers of a positive constant material and a negative dispersive material, and verified the appearance of coupled plasmon-polariton modes of electric and magnetic natures. The photonic dispersion was calculated from Maxwell's equations using the transfer-matrix approach, with the LHM modeled by Drude-like dielectric and magnetic responses. In the case of oblique $\theta \neq 0$ incidence, the photonic dispersion indicates that the magnetic or electric field in the frequency region around the $\langle n(\omega)\rangle = 0$ zeroth order bandgap leads to coupled magnetic or electric plasmon-polariton modes for the TE and TM configurations, respectively. Moreover, present results show that the coupling of light with plasmons is weakened by choosing the plasma frequency inside the zeroth order gap. As light propagation is forbidden in that particular gap-frequency region, the coupled plasmon-polariton mode becomes essentially a pure plasmon mode. This feature permits one to select which type of plasmon polariton (i.e., electric or magnetic) one is willing to excite, by choosing the magnetic or electric plasmon frequency within the zeroth order gap. Here, one might conjecture that the possibility of excitation of magnetic plasmon polaritons might provide a new avenue to the implementation of novel techniques and devices based on the interplay of photonics and magnetism at the nanoscale, similarly to the interplay of photonics and electronics. Therefore, the implementation of plasmonic chips for high data rate processing or efficient sensing applications might also be obtained based on the excitation of magnetic plasmon polaritons. Finally, we have studied an ideal system in which losses have been neglected, and future work including such effects is certainly forthcoming.

Acknowledgments

We are grateful to the Brazilian Agencies CNPq, FAPESP, FAPERJ, and FUJB, the Colombian Agency COLCIENCIAS, and CODI - Univ. of Antioquia for partial financial support.

[1] R. A. Shelby, D. R. Smith, and S. Schultz, Science **292**, 77 (2001).
[2] W. L. Barnes, A. Dereux and T. W. Ebbesen, Nature **424**, 824 (2003).
[3] S. A Maier and H. A. Atwater, J. Appl. Phys. **98**, 011101 (2005).
[4] A. Ramakrishna, Rep. Prog. Phys. **68**, 449 (2005).
[5] E. Ozbay, Science **311**, 189 (2006).
[6] G. Dolling, C. Enkrich, M. Wegener, C. M. Soukoulis, and S. Linden, Opt. Lett. **31**, 1800 (2006).
[7] T. Li, J.-Q. Li, F.-M. Wang, Q.-J. Wang, H. Liu, S.-N. Zhuy and Y.-Y. Zhu, Appl. Phys. Lett. **90**, 251112 (2007).
[8] M. Dragoman and D. Dragoman, Prog. Quant. Electr. **32**, 1 (2008).
[9] J. Pacheco, Jr., T. M. Grzegorczyk, B.-I. Wu, Y. Zhang, and J. A. Kong, Phys. Rev. Lett. **89**, 257402 (2002).
[10] G. V. Eleftheriades, A. K. Iyer, and P. C. Kremer, IEEE Trans. Microwave Theory Tech. **50**, 2702 (2002).
[11] A. Grbic and G. V. Eleftheriades, J. Appl. Phys. **92**, 5930 (2002); L. Liu, C. Caloz, C. C. Chang, and T. Itoh, J. Appl. Phys. **92**, 5560 (2002).
[12] J. Li, L. Zhou, C. T. Chan, and P. Sheng, Phys. Rev. Lett. **90**, 083901 (2003).
[13] H. Jiang, H. Chen, H. Li, Y. Zhang, and S. Zhu, Appl. Phys. Lett. **83**, 5386 (2003).
[14] D. R. Smith, W. J. Padilla, D. C. Vier, S. C. Nemat-Nasser, and S. Schultz, Phys. Rev. Lett. **84**, 4184 (2000).
[15] M. Liscidini and L. C. Andreani, Phys. Rev. E **73**, 016613 (2006).
[16] S. B. Cavalcanti, M. Dios-Leyva, E. Reyes-Gómez, and L. E. Oliveira, Phys. Rev. B **74**, 153102 (2006); *ibid.*, Phys. Rev. E **75**, 026607 (2007); A. Bruno-Alfonso, E. Reyes-Gómez, S. B. Cavalcanti, and L. E. Oliveira, Phys. Rev. A **78**, 035801 (2008).
[17] I. V. Shadrivov, A. A. Sukhorukov, and Y. S. Kivshar, Appl. Phys. Lett. **82**, 3820 (2003).
[18] R. W. Ziolkowski, Phys. Rev. E **70**, 046608 (2004).
[19] H. Daninthe, S. Foteinopoulou, and C. M. Soukoulis, Photonics and Nanostruct. Fundam. Appl. **4**, 123 (2006).
[20] Y. Yuan, L. Ran, J. Huangfu, H. Chen, l. Shen, and J. A. Kong, Opt. Express **14**, 2220 (2006).
[21] M. S. Vasconcelos, P. W. Mauris, F. F. de Medeiros, and E. L. Albuquerque, Phys. Rev. B **76**, 165117 (2007).
[22] Y. Weng, Z-G. Wang, and H. Chen, Phys. Rev. E **75**, 046601 (2007).
[23] L. Zhang, Y. Zhang, L. He, Z. Wang, H. Li, and H. Chen, J. Phys. D: Appl. Phys. **40**, 2579 (2007).